Proc. Natl. Acad. Sci. USA
Vol. 93, pp. 14338–14343, December 1996
Applied Biological Sciences

Protein engineering of *Bacillus thuringiensis* δ-endotoxin: Mutations at domain II of CryIAb enhance receptor affinity and toxicity toward gypsy moth larvae

(insecticidal crystal protein/receptor binding/site-directed mutagenesis)

FRANCIS RAJAMOHAN*, OSCAR ALZATE†, JEFFREY A. COTRILL*, APRIL CURTISS*, AND DONALD H. DEAN*†‡

*Department of Biochemistry, and †Biophysics Program, The Ohio State University, Columbus, OH 43210-1292

Communicated by Arnold L. Demain, Massachusetts Institute of Technology, Cambridge, MA, October 2, 1996 (received for review June 26, 1996)

ABSTRACT **Substitutions or deletions of domain II loop residues of *Bacillus thuringiensis* δ-endotoxin CryIAb were constructed using site-directed mutagenesis techniques to investigate their functional roles in receptor binding and toxicity toward gypsy moth (*Lymantria dispar*). Substitution of loop 2 residue N372 with Ala or Gly (N372A, N372G) increased the toxicity against gypsy moth larvae 8-fold and enhanced binding affinity to gypsy moth midgut brush border membrane vesicles (BBMV) ≈4-fold. Deletion of N372 (D3), however, substantially reduced toxicity (>21 times) as well as binding affinity, suggesting that residue N372 is involved in receptor binding. Interestingly, a triple mutant, DF-1 (N372A, A282G and L283S), has a 36-fold increase in toxicity to gypsy moth neonates compared with wild-type toxin. The enhanced activity of DF-1 was correlated with higher binding affinity (18-fold) and binding site concentrations. Dissociation binding assays suggested that the off-rate of the BBMV-bound mutant toxins was similar to that of the wild type. However, DF-1 toxin bound 4 times more than the wild-type and N372A toxins, and it was directly correlated with binding affinity and potency. Protein blots of gypsy moth BBMV probed with labeled N372A, DF-1, and CryIAb toxins recognized a common 210-kDa protein, indicating that the increased activity of the mutants was not caused by binding to additional receptor(s). The improved binding affinity of N372A and DF-1 suggest that a shorter side chain at these loops may fit the toxin more efficiently to the binding pockets. These results offer an excellent model system for engineering δ-endotoxins with higher potency and wider spectra of target pests by improving receptor binding interactions.**

The use of biological insecticides is favorable because they kill undesirable agricultural and household pests and vectors of human and animal diseases without introducing toxic and nonbiodegradable substances into the ecosystem. The proteinaceous δ-endotoxins produced by the bacterium *Bacillus thuringiensis* are insecticidal to larval forms of several insects belonging to the orders Lepidoptera, Diptera, and Coleoptera (1). Upon ingestion, the CryIA-type crystals are solubilized in the alkaline pH (pH 10–12) of the lepidopteran midgut and activated into a toxin form (60–65 kDa) by gut proteases. The activated toxin then binds to specific receptors located on the apical membrane of epithelial cells lining the midgut (2). The bound toxin might then undergo a conformational change, insert into the epithelial membrane and generate ion channels or pores across the membrane (3–5). The massive disruption of transmembrane potential rapidly kills the midgut cells and leads to the death of the insect (6).

Several *in vitro* studies with labeled toxin and brush border membrane vesicles (BBMV) prepared from target insect midguts have demonstrated that binding of the toxin to midgut receptor plays a key role in insect specificity and toxicity (2, 7, 8). Recent studies have further established a direct correlation between toxicity and irreversible toxin–membrane association (9–12). A 120-kDa CryIAc toxin-binding glycoprotein, aminopeptidase N, has been identified and cloned from *Manduca sexta* and *Heliothis virescens* midgut cells (13, 14). In contrast, CryIAa and CryIAb toxins recognize a 210-kDa protein in *M. sexta* and gypsy moth midgut vesicles (10, 15, 16). The x-ray crystal structure of CryIAa toxin shows a protein composed of three distinct domains (17). Mutational analysis suggests that domain I (residues 33–253) is involved in ion channel activity (18) and domain II (residues 265–461) is involved in receptor recognition to several lepidopteran insects (10, 11). The function of domain III (residues 463–609) is associated with receptor binding (19, 20), ion channel formation (21, 22), and insect specificity (23, 24).

Ge *et al.* (25) demonstrated that the insect specificity between two homologous Cry toxins (CryIAa and CryIAc) could be almost completely exchanged by switching a small hypervariable region of the *cry* genes. The narrow insect specificity of δ-endotoxins could be determined either by specific toxin binding protein(s) located in insect midgut or by functionally distinct epitopes located at the hypervariable regions of toxins. From our earlier studies, we deduced the functional role of the domain II surface exposed loop residues of CryIA and CryIIIA toxins. In CryIAb, the loop 2 residues ^{368}RR^{369} are involved in initial receptor recognition, whereas F371 and G373 are involved in irreversible association of the toxin to the BBMV prepared from *M. sexta* larvae (10, 11). With *H. virescens*, however, loop 2 and loop 3 residues of CryIAb are involved in initial receptor binding (11, 26). The initial receptor binding process was suggested to be mediated by hydrophobic and electrostatic interactions (11, 26). In CryIIIA, loop 1 and 3 residues are suggested to be involved in initial and irreversible binding, respectively, to the midgut vesicles from *Tenebrio molitor* (27). Though the loop residues are broadly considered to be involved in receptor binding, the functional interactions of individual residues differ significantly between target insects or receptors. For example, CryIAb loop 2 mutant F371A decreases the toxicity to *M. sexta* by affecting the irreversible binding, but the same mutant affects neither toxicity nor binding to *H. virescens* (11). Likewise, although CryIAb recognizes different receptors in *M. sexta* (210 kDa) and *H. virescens* (170 kDa) BBMV, alanine substitution of loop 3 residues G439 and F440 affect the initial receptor binding and toxicity in both the insects (26). As a result, these loops are excellent targets for genetic redesigning of more potent toxins with diverse insect specificity.

The publication costs of this article were defrayed in part by page charge payment. This article must therefore be hereby marked "*advertisement*" in accordance with 18 U.S.C. §1734 solely to indicate this fact.

Abbreviation: BBMV, brush border membrane vesicles.

‡To whom reprint requests should be addressed. e-mail: Dean.10@osu.edu.

In this study, point mutations were introduced into the loop regions of CryIAb toxin to explore the role of these residues in toxicity and receptor interaction toward an economically important pest, the gypsy moth. About 311 million acres of forest land is at risk from defoliation by gypsy moth in the United States alone. Our results showed that loop residues N372 and ^{282}AL^{283} play a vital role in receptor binding. Substitutions of these residues with A372 and ^{282}GS^{283}, respectively, have significantly improved (36-fold) the toxicity. The improved toxicity was directly attributable to enhanced binding affinity to the receptor molecule. These results strongly suggest the possibility of engineering novel δ-endotoxins with higher activity and wider host spectra to meet the needs of the agricultural industry.

MATERIALS AND METHODS

Bacterial Strains and Construction of Mutants. *Escherichia coli* containing *B. thuringiensis* δ-endotoxin gene *cryIAb (cryIAb9-033)* was obtained from T. Yamamoto (Sandoz Agro Inc., Palo Alto, CA). Uracil-containing template of *cryIAb* was obtained by transforming *E. coli* CJ236 with pSB033b (10). The primers used for oligonucleotide-directed mutagenesis were provided by Sandoz Agro Inc. Site-directed mutagenesis procedure was as described in the manufacturer's manual (Muta-Gene M13 *In Vitro* Mutagenesis Kit; Bio-Rad). Single-stranded DNA sequencing was carried out by the method of Sanger *et al*. (28), following the manufacturer's (United States Biochemical) instructions. Mutants N372A and N372G were constructed by substituting domain II loop 2 residue N372 of CryIAb toxin with Ala and Gly, respectively. Mutant D3 is a deletion of residue N372 from CryIAb toxin. The triple mutant, DF-1, is a substitution of residues ^{282}AL^{283} (located in domain II, between α-helix 8a and α-helix 8) of N372A mutant with ^{282}GS^{283}.

Expression Purification and Solubilization of Toxins. Wild-type and mutant δ-endotoxins were expressed in *E. coli* MV1190 and purified as described before (10). The final pellet, referred to as the crystal, was solubilized in crystal solubilization buffer (50 mM Na_2CO_3, pH 9.5/10 mM DTT) for 3 h at 37°C. The solubilized crystal protein was referred to as the protoxin. Activation of the protoxin was carried out by treating the protoxin with 2% (by mass) trypsin at 37°C for 5 h and dialysis overnight against 50 mM sodium carbonate buffer (pH 9.5). Protein concentration of the samples was estimated using protein assay reagents (Pierce), and the purity was analyzed by SDS/10% PAGE.

Iodination of Toxin. Iodination of trypsin-activated toxins was performed as described (10). In brief, 25 μg of toxin were iodinated using one IODO-BEAD (Pierce) and 1 mCi (1 Ci = 37 GBq) of Na^{125}I, as instructed by the manufacturer (Pierce). The free iodine was separated from the toxin by passing the sample through a 2.0-ml Excellulose column (Pierce). The specific activities of the labeled CryIAb, N372A, N372G, DF-1, and D3 proteins were 0.52, 0.37, 0.36, 0.53, and 0.48 mCi/mg, respectively.

Preparation of BBMV. Midguts from fourth instar gypsy moth larva were isolated as described previously (21). BBMV were prepared by the differential magnesium precipitation method modified by Wolfersberger *et al.* (29). The final pellet, referred to as BBMV, was resuspended in binding buffer (8 mM $NaHPO_4$/2 mM KH_2PO_4/150 mM NaCl, pH 7.4) to a final protein concentration of 1 mg/ml.

Binding Assays. Saturation binding assays were performed by incubating ^{125}I-labeled toxin (1 nM) with increasing amounts (2.5 to 200 μg/ml) of BBMV. After 1 h of incubation at room temperature, the samples were centrifuged and the radioactivity in the pellet was measured as described (10).

Competition binding was performed by incubating 200 μg of BBMV per ml and 1 nM ^{125}I-labeled toxin with increasing concentrations (0–500 nM) of the same (homologous) or different (heterologous) nonlabeled protein as competitor. The reaction mixture was incubated at room temperature for 1 h, and the unbound toxin was separated from the bound toxin by centrifugation as described (10). The radioactivity in the final pellet was measured in a gamma counter (Beckman). The binding site concentrations (B_{max}) and binding affinity (K_{com}) were analyzed (27) by using the LIGAND computer program (30).

Dissociation binding assays were performed as described (10). ^{125}I-labeled toxin (1.0 nM) was incubated with 20 μg of BBMV per 100 μl for 1 h at room temperature to achieve saturation binding. Corresponding nonlabeled toxin (100 nM final concentration in 20 μl) was then added to each sample tube and continued the incubation (postincubation or dissociation reaction). The reaction was stopped at different time intervals (10 min to 1 h) by centrifugation. The toxin bound to BBMV was measured as described (10). Toxin binding autoradiography was performed as described (11).

Voltage Clamp Analysis. Voltage clamp experiments were performed as described by Chen *et al.* (21). Fifth instar gypsy moth larvae were used and the dissection and mounting of midgut membrane were as described by Harvey *et al.* (31). After 15 min of stabilization, 6.5 ng of trypsin-activated toxin per ml was injected into the lumen side of the chamber. The drop in short circuit current (I_{sc}) was tracked with a Kipp & Zonen (Delft, The Netherlands) recorder, and the data were collected with the MacLab data acquisition system.

Ligand Blot. A total of 40 μg of BBMV proteins was solubilized in Laemmli sample buffer (32), separated by SDS/6% PAGE, and transferred onto polyvinylidene difloride membrane as described (33). The blots were treated separately with ^{125}I-labeled CryIAb, N372A, and DF-1 toxins (3 nM) and developed as described (10).

Immunoblotting. Gypsy moth gut enzyme digestion of the toxins was performed by incubating 5 μg of toxin with freshly prepared gut juice (the gut fluid vomited by the larvae upon very gentle squeezing) in 50 mM sodium carbonate buffer (pH 9.5) at 37°C for 1 h (10). The reaction was stopped and examined as described before (10).

Thermal Denaturation and CD Analysis of Toxins. Thermal denaturation and CD spectra of trypsin-activated toxins were performed with a Spex CD6 spectrophotometer (Jobin-Yvon, Longjumeau, France) using a 1-cm pathlength quartz cell (Uvonic Instruments, Plainview, NY). Temperature gradients (40–85°C) were created with a HP89090A Peltier temperature controller (Hewlett–Packard) and a circulating water bath (Lauda RC6; Brinkmann Instruments, Westbury, NY). Heating and cooling were controlled in steps of 2°C with 20 min of equilibration time, and CD spectra were recorded at a fixed wavelength of 222 nm and recorded on CD6 software supplied by Jobin-Yvon. Transition curves were normalized to the fraction of the protein folded using the standard equation: $F = ([\theta] - [\theta]_u)/([\theta]_n - [\theta]_u)$, where $[\theta_n$ and $[\theta]_u$ represent the ellipticity values for fully folded and unfolded proteins, respectively, and $[\theta]$ is the observed ellipticity at 222 nm (34). A protein concentration of 0.2 mg/ml in 10 mM sodium carbonate buffer (pH 10.5) with 0.1 M guanidine hydrochloride (Boehringer Mannheim) was used for CD analysis.

Toxicity Assays. Gypsy moth eggs were kindly supplied by Gary Bernon (U.S. Department of Agriculture, Otis Methods Development Center, Beltsville, MD) and reared on artificial diet (Bio-serv, Frenchtown, NJ). Bioassays were essentially performed as described by Rajamohan *et al.* (11). Protein samples were diluted in 50 mM sodium carbonate buffer (pH 9.5), and 100-μl samples were applied per well (2 cm^2) on an artificial diet in 24-well tissue culture plates. Two neonate (3- to 5-day-old) larvae were placed on each well and insect mortality was recorded after 5 days. At least five concentrations for each protein were used for the calculation of LC_{50}

(50% lethal concentration) value, and 25–30 larvae were used per each concentration. Force feeding bioassays on fourth instar gypsy moth larvae were performed as detailed in Rajamohan *et al.* (26). Three sets of ten larvae were used for each toxin concentration (at least five concentrations per toxin), and the dosed larvae were then fed on artificial diet (Bio-serv). Control insects were dosed with same volume of 50 mM sodium carbonate (pH 9.5). Toxicity was assessed after 5 days and the 50% growth inhibition dosage (ID_{50}) was obtained by probit analysis (35).

RESULTS

Expression and Stability of Mutant Toxins. Wild-type (CryIAb) and mutant δ-endotoxins were solubilized and the protoxins were analyzed on a SDS/10% PAGE (Fig. 1*A*). The wild type and mutants (N372A, N372G, D3, and DF-1) produced a 130-kDa protoxin, and the yields were comparable. After treatment with trypsin, all the mutant proteins produced a stable 65-kDa toxin similar to that of wild type (Fig. 1*B*). Stability of the mutant proteins to insect gut enzymes was analyzed by treating the toxins with freshly prepared gypsy moth gut juice. Both wild type and mutants were activated into a 60-kDa stable toxin form (Fig. 1*C*). Thermal denaturation of the toxins was performed to investigate whether the mutations introduced any changes in stability of the toxin molecule. Our analysis showed that the average melting temperature (T_m) for all the toxins is 58 ± 3.5°C, suggesting that these changes in toxicity were not caused by structural alterations of the toxin molecule (Fig. 2).

Biological Activity Toward Gypsy Moth. The potency of wild-type and mutant toxins toward neonate (3–5 days old) and fourth instar larvae were compared and are presented in Table 1. On neonates larvae, mutant toxins DF-1, N372A, and N372G were 36-, 8.5-, and 8.3-fold more toxic, respectively, than the wild-type toxin. While the toxicity of mutants N372A and N372G (LC_{50} values 34 and 35 ng/cm^2, respectively) were comparable, they were 4.4 times less toxic than DF-1 toxin (LC_{50} = 8.0 ng/cm^2). Mutant D3 (deletion of N372) substantially lost toxicity (LC_{50} = >6000 ng/cm^2) to neonates (Table 1). The mutant DF-1 was 4-fold more toxic than CryIAa, the most potent toxin to gypsy moth (Table 1).

On fourth instar larvae, mutant toxin DF-1 was 17-fold more toxic than the wild-type toxin (Table 1). While the mutant toxins N372A and N372G were 10-fold more active than the wild-type, they were ≈1.8 times less active than DF-1 toxin. The toxicity of mutant D3 was greatly reduced and was not toxic up to a concentration of 10,000 ng per larvae (Table 1).

Binding of Toxins to Gypsy Moth BBMV Proteins. Saturation binding data showed that the binding of the toxins was specific and saturable. Binding of ^{125}I-labeled toxins increased with increasing concentrations of BBMV from 2.5 to 200 μg/ml BBMV (Fig. 3). Binding of ^{125}I-labeled toxin in the presence of corresponding excess nonlabeled ligand (nonspecific binding) was subtracted from the total binding at each data point (Fig. 3). The total amount of toxins bound to 200 μg of vesicle protein per ml were 0.9, 1.3, and 4.1 ng of CryIAb, N372A and DF-1 toxins, respectively. Mutant D3, however, showed only a weak binding (0.15 ng toxin) to the vesicles. Competition binding of wild-type and mutant toxins to gypsy moth BBMV proteins were carried out by homologous (data not shown) and heterologous competition binding assays. When ^{125}I-labeled CryIAb was put into competition with nonlabeled toxins, mutant DF-1 competed with highest binding affinity for the binding sites of labeled toxin and was followed by other toxins in the order of N372A, N372G, and CryIAb, respectively (Fig. 4). Mutant toxin D3, however, competed only marginally for the binding sites of CryIAb toxin. The binding affinities (K_{com}) of the toxins calculated from homologous competition binding assays are given in Table 1. The binding affinity of DF-1 was 18.6, 4.2, and 4.6 times higher than CryIAb, N372A, and N372G toxins, respectively. The binding site concentrations (B_{max}) of N372A and N372G were comparable (11.2–12.6 pmol), whereas the B_{max} of CryIAb (8.3 pmol) was 1.4, 1.4, and 2.0 times lower than N372A, N372G, and DF-1, respectively. The K_{com} and B_{max} values of mutant D3 were not determined, due to its weak interaction with gypsy moth BBMV (Table 1).

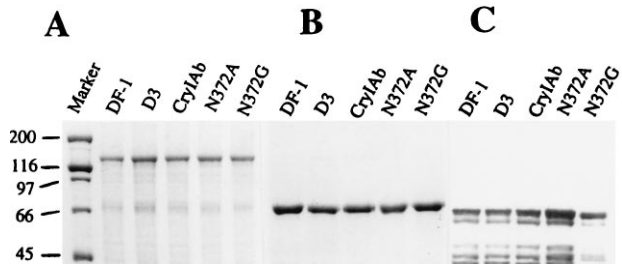

FIG. 1. Comparison of the yields and stability of wild-type CryIAb and mutant δ-endotoxins on SDS/10% PAGE. (*A*) Protoxins, (*B*) trypsin-activated toxins, and (*C*) Western blot analysis of wild-type and mutant toxins after digestion with gypsy moth gut juice are shown. Masses of the protein markers (in kilodaltons) are shown on the left.

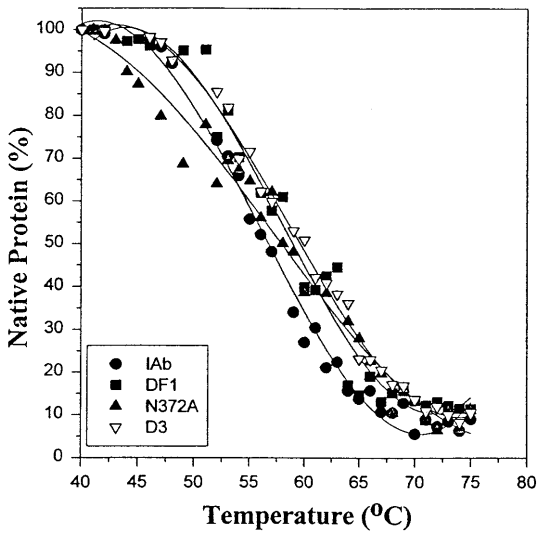

FIG. 2. Comparison of CD spectra of thermally denatured wild-type and mutant toxins. Trypsin-activated toxins were subjected to thermal denaturation in the presence of 0.1 M guanidine hydrochloride and scanned on a Spex CD6 spectrophotometer.

Dissociation Binding Assays. The stability of the BBMV-bound toxins were examined by allowing the ^{125}I-labeled toxins to bind the vesicles to saturation and were then chased with the corresponding nonlabeled toxins. The results showed that 85–90% of the BBMV-bound toxins were irreversibly associated and were not dissociable with addition of 100 times excess corresponding toxin (Fig. 5). However, the net amount of toxins bound to the vesicles differ significantly among the mutants. The amount of D3, CryIAb, N372A, and DF-1 toxins irreversibly bound to the BBMV were 1.2, 14.5, 20.3, and 68.3 fmol, respectively (Fig. 5). Dissociation and autoradiography binding studies revealed that <1% of the input-labeled D3 toxin bound to the BBMV compared with 15, 20, and 68% binding of CryIAb, N372A, and DF-1 toxins, respectively (Fig. 5 and Fig. 5 *Inset*).

Identification of Toxin Binding BBMV Polypeptide. Gypsy moth BBMV proteins were blotted onto polyvinylidene difloride membrane, and the toxin binding protein was identified by incubating the membrane with ^{125}I-labeled CryIAb, N372A, and DF-1 toxins. The labeled CryIAb, N372A, and DF-1 toxins

Table 1. Biological activity, binding constants, and I_{sc} of wild-type and mutant toxins toward gypsy moth

Toxin	Neonates LC_{50},* ng/cm^2	Relative potency†	Fourth instar larva ID_{50},‡ ng/larvae	Relative potency§	K_{com},¶ nM	B_{max},‖ pmol	I_{sc},** μA/min per cm^2
CryIAb	290 (210–350)	1.00	2605 (2000–3050)	1.00	9.3 ± 0.81	8.3 ± 0.9	−4.4 ± 1.2
CryIAa	28 (20–33)	10.36	151 (100–190)	17.25	1.9 ± 0.57	10.3 ± 1.1	−27.3 ± 1.1
N372A	34 (28–41)	8.53	271 (190–301)	9.61	2.1 ± 0.25	11.9 ± 1.3	−24.2 ± 0.9
N372G	35 (27–43)	8.28	274 (210–305)	9.51	2.3 ± 0.30	11.2 ± 0.9	−23.9 ± 1.8
DF-1	8 (6–11)	36.25	149 (91–189)	17.48	0.5 ± 0.08	16.9 ± 1.9	−32.2 ± 1.0
D3	>6000††	>0.05	>10,000††	>0.03	UD	UD	UD

UD, undetectable.
*LC_{50}, 50% lethal concentration. Confidence intervals (95%) are given in parentheses.
†Relative potency, wild-type (CryIAb) LC_{50}/mutant LC_{50}.
‡ID_{50}, dose of toxins that cause growth inhibition in 50% of larvae assayed. Confidence intervals (95%) are in parentheses.
§Relative potency, wild-type (CryIAb) ID_{50}/mutant ID_{50}.
¶K_{com}, dissociation constant (determined from homologous competition binding). Each value is the mean ± SD of three experiments.
‖B_{max}, binding site concentration (determined from homologous competition binding). Each value is the mean ± SD of three experiments.
**I_{sc}, Inhibition of short circuit current. Each value is the mean ± SD of three experiments.
††Insufficient mortality to calculate IC_{50} or ID_{50}.

bound exclusively to a 210-kDa polypeptide under these experimental conditions (Fig. 6).

Voltage Clamping of Gypsy Moth Midgut. The inhibition of short circuit current (I_{sc}) in response to the addition of wild type, and mutant toxins were analyzed and reported in Table 1. I_{sc} measures the active transport of ions from the hemolymph side of the midgut to the lumen side by the ion pumps located in the membrane. The more negative the slope value is, the better the toxin activity. The slope of the I_{sc} inhibition for DF-1, N372A, N372G, and CryIAb were −32.2, −24.2, −23.9, and −4.4 μA/min per cm^2, respectively, at a toxin concentration of 6.5 ng/ml. The slope for CryIAb (−4.4 μA/min per cm^2) was ≈6 times smaller than N372A and N372G (Table 1) toxins. The slope for DF-1 was 7.3 and 1.3 times larger than CryIAb and N372A toxin, respectively (Fig. 7; Table 1). Mutant D3 did not show any measurable inhibition in I_{sc} at this toxin concentration (Fig. 7).

DISCUSSION

Understanding the molecular mechanism that confers insecticidal activity and biological specificity to *B. thuringiensis* δ-endotoxins is a vital step for the rational design of more potent and broader-spectrum toxins. We have previously analyzed the functional roles of loop 2 and loop 3 residues of CryIAb toxin toward *M. sexta* and *H. virescens* (10, 11, 26). In this study, mutants were constructed in domain II surface exposed loops of CryIAb and their functional activity toward gypsy moth (*Lymantria dispar*) larvae were analyzed.

Mutants were constructed at loop 2 of CryIAb toxin by replacing residue N372 with Ala (N372A) and Gly (N372G) and by deleting the residue N372 (D3). All the mutants and wild type expressed a 130- to 135-kDa protoxin and yielded a stable 65- and 60-kDa toxin on treatment with trypsin and gypsy moth gut juice, respectively (Fig. 1). Thermal denaturation of the toxins followed by CD analysis also suggested that the mutations did not affect the structure of the toxin molecule (Fig. 2). Insect bioassays performed with gypsy moth neonates (3–5 days old) and fourth instar larvae indicated that N372A and N372G toxins are ≈8- to 9-fold more toxic than CryIAb, whereas D3 has lost most of its larvicidal activity (Table 1). Binding with ^{125}I-labeled toxins displayed specific and saturable binding to gypsy moth midgut vesicles (Fig. 3). However, toxin N372A binds 1.5 and 9 times more than CryIAb and D3 toxins, respectively, to the same amount of BBMV (Fig. 3).

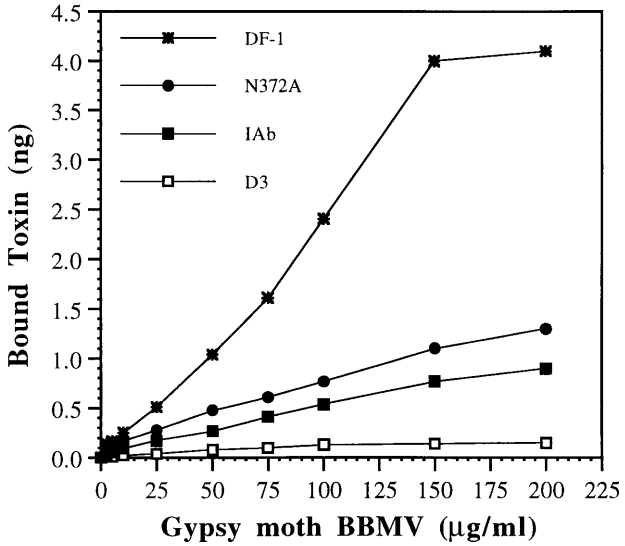

FIG. 3. Saturation binding of ^{125}I-labeled (1 nM) wild-type and mutant toxins. Toxins were labeled as described (8) and were incubated with increasing concentrations of gypsy moth BBMV (2.5 to 200 μg/ml).

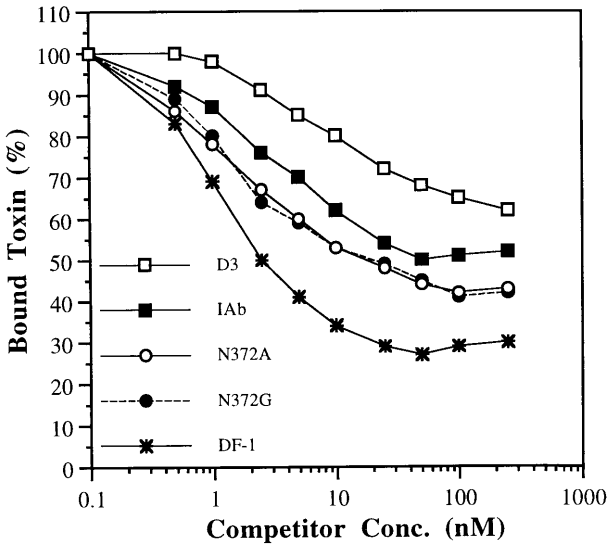

FIG. 4. Heterologous competition binding of ^{125}I-labeled wild-type (1 nM) in the presence of increasing concentrations on nonlabeled CryIAb, N372A, N372G, DF-1, and D3 toxins. Gypsy moth BBMV (200 μg/ml per tube) was used, and each point is an average value of three individual experiments. Binding is expressed as a percentage of the total amount bound upon incubation with labeled toxin.

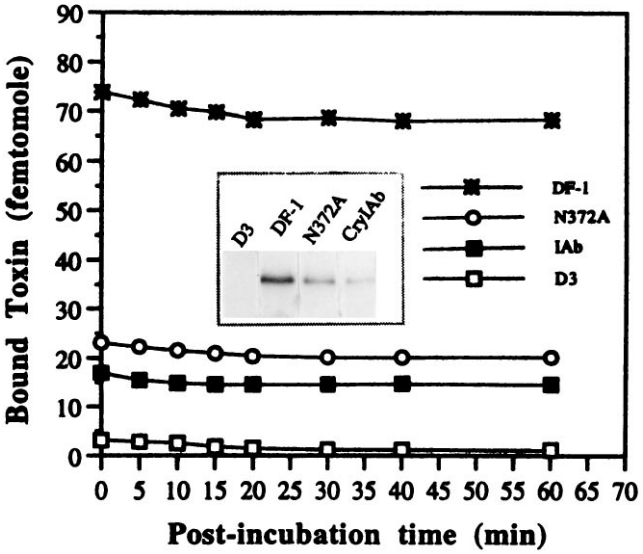

FIG. 5. Dissociation of membrane-bound ^{125}I-labeled wild-type and mutant toxins. Gypsy moth BBMV (20 μg per 100 μl) was incubated with 1 nM labeled toxins (association reaction) for 1 h. At the end of association reaction, 100 nM concentration of corresponding nonlabeled toxin was added to the test samples, and incubation (postbinding) was stopped at different time intervals. Nonspecific binding was obtained by incubating the labeled toxin with BBMV in the presence of a 1000-fold excessive corresponding nonlabeled toxin, and the value was subtracted from the total binding. (*Inset*) BBMV-bound labeled toxins at the end of association binding were resolved on SDS/10% PAGE and autoradiographed. The amounts of DF-1, N372A, CryIAb, and D3 toxins bound to the vesicles were 6050, 2200, 1390, and 321 cpm, respectively.

Heterologous competition bindings using ^{125}I-labeled CryIAb and N372A (data not shown) suggest that there is only one binding site, and the mutant toxins, N372A and N372G, compete with higher binding affinity (4-fold higher) compared with the wild type (Fig. 4; Table 1). Toxin D3, however, competed only marginally for the binding of wild-type toxin. The K_{com} value of toxin D3 was not determined due to its weak binding affinity. These results directly correlate to our bioassay data. Toxins with higher potency (N372A, N372G) exhibit stronger binding, whereas toxins with no or marginal toxicity (D3) show weak binding. Our previous results indicated that alanine substitution of N372 affect neither toxicity nor receptor binding toward *M. sexta*, though CryIAb toxin binds to a 210-kDa receptor in *M. sexta* and gypsy moth (10, 16). The CryIAb binding proteins (210-kDa) of *M. sexta* and gypsy moth may be related but not identical, or they could be two distinct proteins of a similar molecular size. Our results also suggest that a smaller side-chain at residue 372 provides the toxin a closer contact with the binding pocket, which in turn increases the affinity. However, the substantial loss of toxicity by the removal of residue N372 might imply a local alteration in

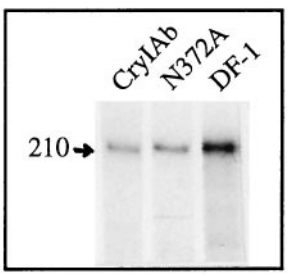

FIG. 6. Binding of ^{125}I-labeled toxins to protein blots of gypsy moth BBMV proteins. A total of 40 μg of BBMV proteins was blotted and probed with 3 nM of labeled toxins.

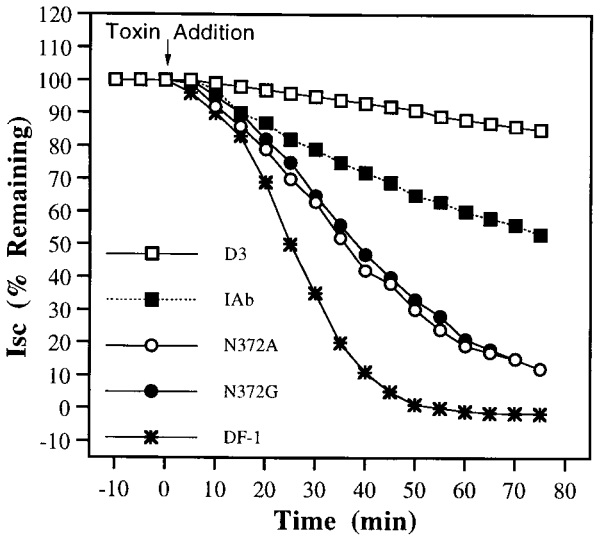

FIG. 7. Inhibition of I_{sc} across gypsy moth midgut by wild-type and mutant toxins. A total of 6.5 ng of toxin per ml was injected into the lumen side of the chamber in separate experiments, and the drop in I_{sc} was measured. The I_{sc} measured before the addition of the toxin was considered as 100%. Each point is an average of three independent experiments.

backbone conformation of the loop, without changing the global structure, preventing the protein from reaching the binding site.

The second mutation was focused at loop residues ^{282}AL^{283} of our CryIAb (CryIAb9-033) toxin located between α-helix 8a and α-helix 8 (17). These residues are replaced by ^{282}GS^{283} in CryIAb2 (a natural variant, which differs from CryIAb9-033 only by these two residues) and was shown to be 10 times more toxic than CryIAb9-033 (M. K. Lee and D.H.D., unpublished data) toward gypsy moth. We have constructed a triple mutant, DF-1, by substituting ^{282}AL^{283} with ^{282}GS^{283} in a N372A background. Therefore, DF-1 toxin differs from CryIAb (CryIAb9-033) toxin only by three amino acids (^{282}GS^{283} and A372). DF-1 toxin is structurally as stable as the wild type when treated with trypsin and gut juice, as well as by thermal denaturation and CD analysis (Figs. 1 and 2). Interestingly, DF-1 toxin is 36 and 17 times more toxic to gypsy moth neonates and fourth instar larvae, respectively, than the wild type. Moreover, DF-1 toxin is 4 times more active than N372A, N372G, and CryIAa (the most potent toxin to gypsy moth) toxins toward neonates (Table 1). Binding assay data showed that toxin DF-1 binds 4.6 and 3.7 times more than wild-type and N372A toxins, respectively (Fig. 3). Heterologous competition binding studies suggested that DF-1 toxin competed more successfully than N372A, N372G, and CryIAb toxins for the binding sites of labeled wild-type toxin (Fig. 4). The binding affinity of DF-1 is 18.6-, 4.2-, and 4.6-fold higher than wild-type, N372A, and N372G toxins, respectively (Table 1). The binding site concentration (B_{max}) of DF-1 is 2-fold higher than wild-type toxin, while it is comparable with N372A and N372G toxins (Table 1).

One possibility to explain this result is that DF-1 could recognize an additional binding site on the same receptor or bind to a different functional receptor with higher affinity. Our protein blotting experiments (Fig. 6) and heterologous binding assays with labeled CryIAb (Fig. 4) and DF-1 (data not shown) strongly indicate that the increased binding and toxicity of mutants (DF-1, N372A, and N372G) is not due to binding to other functional receptor(s). However, binding to additional sites of the same receptor molecule cannot be ruled out. Despite the fact that the interaction of Cry toxins with the BBMV is a two-step process (reversible and irreversible), the

binding site concentrations (B_{max}) calculated from LIGAND program represents both reversibly and irreversibly (or inserted) associated toxin–ligand complexes (12). Therefore, caution should be exercised when interpreting the relationship between B_{max} and toxicity. These results indicate that the potency of mutant N372A is further improved (4-fold) by replacing ^{282}AL^{283} with ^{282}GS^{283} and is directly correlated with a 4.4-fold improved binding affinity.

Recently, several studies have suggested a direct correlation between toxicity and irreversible association of the toxin to the vesicles rather than initial binding affinity (10–12). Therefore, we performed dissociation binding to evaluate whether the enhanced activity of the mutants was related to better irreversible membrane association. In the dissociation binding assay, ≈85-90% of the BBMV-bound toxins are irreversibly associated to the vesicles, regardless of the total bound toxin. However, there is a direct correlation between binding affinity and total amount of toxin irreversibly associated to the vesicles (Fig. 5). A toxin with higher binding affinity (DF-1) exhibits more binding (68 fmol), whereas toxins with lower (N372A, CryIAb) or very little (D3) binding affinity bind less (20.3, 15, and 1.2 fmol, respectively). Alternatively, receptor-bound toxin molecules could facilitate additional toxin–toxin interaction, then insert into the membrane as oligomers. Hence, the higher binding of DF-1 mutant could be caused by a better toxin–toxin interaction. When we immobilized the toxin on a solid surface and probed with corresponding labeled toxin, there was no noticeable toxin–toxin interaction among CryIAb, N372A, and DF-1 toxins (data not shown). However, a ligand-induced oligomerization at the surface of the membrane cannot be ruled out.

Our previous result suggested the involvement of charged (^{368}RR^{369}) and an aromatic residue (F371) in initial and irreversible binding of CryIAb toxin, respectively, to *M. sexta* BBMV (10, 11). Taken together, these results imply that toxin–receptor interaction is complex and needs further investigation. The relationship between binding affinity and toxicity is further strengthened by voltage clamping experiments with gypsy moth midgut membrane. The toxins that have greater irreversible binding and binding affinity inhibit the I_{sc} more efficiently than the toxins with quantitatively less irreversible binding and binding affinity (Fig. 7).

In summary, our experimental approach to identify the receptor binding toxin residues and to improve the binding affinity using site-directed mutagenesis techniques has substantially enhanced the potency of CryIAb toxin. Our data identify the residues N372 and ^{282}AL^{283} of CryIAb toxin as part of gypsy moth 210-kDa receptor binding epitope. Substitution of residues N372 and ^{282}AL^{283} with smaller (A372) and less hydrophobic residues (^{282}GS^{283}) have significantly enhanced the toxin–receptor contact and subsequently improved the binding affinity and potency. These second-generation mutant proteins could be successfully used to express in transgenic plants and to delay the *B. thuringiensis* resistance in insects. This protein engineering approach could also be effectively used as a model system in strain improvement and development of highly active and broader pest specificity toxins.

We thank Daniel R. Zeigler, Mi K. Lee, S. J. Wu, and S. R. Hussain for their critical evaluation and Takashi Yamamoto (Sandoz Agro Inc.) for preparing the mutagenic oligonucleotides. We are grateful to David Stetson (Department of Zoology, The Ohio State University) for the use of the voltage clamp apparatus. O.A. has a fellowship from the Colombian Institute for the Advancement of Science (COLCIENCIAS). This work was supported by Grant RO1 AI 29092 from the National Institutes of Health to D.H.D.

1. Yamamoto, T. & Powell, G. K. (1993) in *Advanced Engineered Pesticides*, ed. Kim, L. (Dekker, New York), pp. 3–42.
2. Hofmann, C., Lüthy, P., Hutter, R. & Pliska, V. (1988) *Eur. J. Biochem.* **173,** 85–91.
3. Lorence, A., Darszon, A., Díaz, C., Liévano, A., Quintero, R. & Bravo, A. (1995) *FEBS Lett.* **360,** 217–222.
4. Schwartz, J.-L., Garneau, L., Masson, L. & Brousseau, R. (1991) *Biochim. Biophys. Acta* **1065,** 250–260.
5. Martin, G. F. & Wolfersberger, M. G. (1995) *J. Exp. Biol.* **198,** 91–96.
6. Wolfersberger, M. G. (1992) *J. Exp. Biol.* **172,** 377–386.
7. Van Rie, J., McGaughey, W. H., Johnson, D. E., Barnett, B. D. & Van Mellaert, H. (1990) *Science* **247,** 72–74.
8. Hofmann, C., Vanderbruggen, H., Höfte, H., Van Rie, J., Jansens, S. & Van Mellaert, H. (1988) *Proc. Natl. Acad. Sci. USA* **85,** 7844–7848.
9. Ihara, H., Kuroda, E., Wadano, A. & Himeno, M. (1993) *Biosci. Biotechnol. Biochem.* **57,** 200–204.
10. Rajamohan, F., Alcantara, E., Lee, M. K., Chen, X. J. & Dean, D. H. (1995) *J. Bacteriol.* **177,** 2276–2282.
11. Rajamohan, F., Cotrill, J. A., Gould, F. & Dean, D. H. (1996) *J. Biol. Chem.* **271,** 2390–2396.
12. Liang, Y., Patel, S. S. & Dean, D. H. (1995) *J. Biol. Chem.* **270,** 24719–24724.
13. Sangadala, S., Walters, F. S., English, L. H. & Adang, M. J. (1994) *J. Biol. Chem.* **269,** 10088–10092.
14. Gill, S. S., Cowles, E. A. & Francis, V. (1995) *J. Biol. Chem.* **270,** 27277–27282.
15. Vadlamudi, R. K., Ji, T. H. & Bulla, L. A., Jr. (1991) *J. Biol. Chem.* **268,** 12334–12340.
16. Lee, M. K. & Dean, D. H. (1996) *Biochem. Biophys. Res. Commun.* **220,** 575–580.
17. Grochulski, P., Masson, L., Borisova, S., Pusztai-Carey, M., Schwartz, J. L., Brousseau, R. & Cygler, M. (1995) *J. Mol. Biol.* **254,** 447–464.
18. Walters, F., Slatin, S. L., Kulesza, C. A. & English, L. H. (1993) *Biochem. Biophys. Res. Commun.* **196,** 921–926.
19. Aronson, A. I., Wu, D. & Zhang, C. (1995) *J. Bacteriol.* **177,** 4059–4065.
20. Lee, M. K., Young, B. A. & Dean, D. H. (1995) *Biochem. Biophys. Res. Commun.* **216,** 306–312.
21. Chen, X. J., Lee, M. K. & Dean, D. H. (1993) *Proc. Natl. Acad. Sci. USA* **90,** 9041–9045.
22. Wolfersberger, M. G., Chen, X. J. & Dean, D. H. (1996) *Appl. Environ. Microbiol.* **62,** 279–282.
23. Ge, A. Z., Rivers, D., Milne, R. & Dean, D. H. (1991) *J. Biol. Chem.* **266,** 17954–17958.
24. De Maagd, R. A., Kwa, M. S. G., Van Der Klei, H., Yamamoto, T., Schipper, B., Vlak, J. M., Stiekema, W. J. & Bosch, D. (1996) *Appl. Environ. Microbiol.* **62,** 1537–1543.
25. Ge, A. Z., Shivarova, N. I. & Dean, D. H. (1989) *Proc. Natl. Acad. Sci. USA* **86,** 17954–17958.
26. Rajamohan, F., Hussain, S. R. A., Cotrill, J. A., Gould, F. & Dean, D. H. (1996) *J. Biol. Chem.* **271,** 25220–25226.
27. Wu, S. J. & Dean, D. H. (1996) *J. Mol. Biol.* **255,** 628–640.
28. Sanger, F. A., Nicklen, A. & Coulson, A. R. (1977) *Proc. Natl. Acad. Sci. USA* **74,** 5463–5467.
29. Wolfersberger, M. G., Lüthy, P., Maure, A., Parenti, P., Sacchi, V. F., Giordana, B. & Hanozet, G. M. (1987) *Comp. Biochem. Physiol. A Physiol.* **86,** 301–308.
30. Munson, P. J. & Rodbard, D. (1980) *Anal. Biochem.* **107,** 220–239.
31. Harvey, W. R., Crawford, D. N. & Spaeth, D. D. (1990) *Methods Enzymol.* **192,** 599–608.
32. Laemmli, U. K. (1970) *Nature (London)* **227,** 680–685.
33. Lu, H., Rajamohan, F. & Dean, D. H. (1994) *J. Bacteriol.* **176,** 5554–5559.
34. Woody, R. W. (1995) *Methods Enzymol.* **246,** 34–71.
35. Raymond, M. (1985) *ORSTROM Ser. Entomol. Mer. Parasitol.* **22,** 117–121.